Wärme- und Stoffübertragung 27, 225–231 (1992)

Wärme- und Stoffübertragung

Determination of specific heat and true thermal conductivity of glass from dynamic temperature data *

D. Mann; R. E. Field; and **R. Viskanta,** West Lafayette, IN, USA

Abstract. A method to determine the true specific heat and true thermal conductivity for glass and other semitransparent materials from dynamic temperature data is presented. A unique fabrication technique to obtain high quality dynamic temperature data from glass test plates employing thermocouples fused to the glass is described. The true thermal conductivity and specific heat of float glass has been measured using these techniques, and the results are compared with the scant data available in the literature. Sensitivity of the measured specific heat and thermal conductivity to sources of uncertainty is identified and these are discussed.

Bestimmung der spezifischen Wärmekapazität und der wahren Wärmeleitfähigkeit von Glas aus dynamischen Temperaturverläufen

Zusammenfassung. Eine Methode zur Bestimmung der wahren spezifischen Wärmekapazität und der Wärmeleitfähigkeit von Glas und anderen semitransparenten Materialien aus dynamischen Temperaturverläufen wird vorgestellt. Es wird eine außergewöhnliche Herstellungstechnik beschrieben, die in das Glas eingeschmolzene Thermoelemente verwendet, um genaue dynamische Temperaturmeßwerte zu erhalten. Die wahre Wärmeleitfähigkeit und die spezifische Wärmekapazität von Floatglas wurde mit dieser Technik gemessen. Die Ergebnisse werden mit den spärlichen verfügbaren Daten aus der Literatur verglichen. Die Empfindlichkeit der gemessenen spezifischen Wärmekapazität und Wärmeleitfähigkeit gegenüber Fehlerquellen wurde erkannt und diskutiert.

Nomenclature

c	specific heat
c_0	speed of light in a vacuum
E	internal energy
F	radiant flux
f	blackbody fraction
h	convective heat transfer coefficient or Planck's constant
$I_{b\lambda}$	Planck's function, $2h\,c_0^2/\lambda^5\,[\exp(h\,c_0/k\,T)-1]$
k	thermal conductivity or Boltzmann's constant
L	thickness of layer of semitransparent plate
m	mass
T	temperature
t	time
y	y-direction coordinate
α	absorptivity
ε	emissivity
ν	frequency
ϱ	reflectivity or density

Subscripts

a	ambient temperature
s	refers to plate surface
w	refers to surroundings
1	refers to the interface between a semitransparent solid and surrounding medium
2	refers to the interface between a semitransparent solid and surrounding medium
λ	refers to wavelength
ν	refers to frequency

1 Introduction

Control of the temperature distribution within the plate is very important during production, fabrication, and heat-treatment of flat glass. The need to determine and control the plate temperature in the glass manufacturing has been well documented in the literature [1–4]. At the temperatures required for glass fabrication processes, its semitransparent nature produces an internal radiative energy transfer component which dominates the energy transfer from the glass to the surroundings. The radiant energy exchange within the plate substantially increases the complexity of the energy accounting required to model production and fabrication processes.

In glass, the energy transfer occurs by both molecular diffusion through lattice waves (phonons) and the emission and absorption of electromagnetic energy (photons). Analysis of the temperatures within semitransparent materials requires rigorous accounting of both radiative transfer and molecular diffusion. Accurate specification of four intrinsic properties of glass are also needed to obtain successful results from an energy equation model. The required intrinsic properties are: 1) true molecular thermal conductivity, 2) true specific heat, 3) the spectral absorption coefficient, and 4) both (real and imaginary) index of refraction components.

Of these four properties the true thermal conductivity is the most difficult to determine. A plethora of data for the thermal conductivity of glasses exists in the literature (e.g., see

* Dedicated to Prof. Dr.-Ing. U. Grigull's 80th birthday

Touloukian et al. [5]), but rarely has there been an attempt to separate radiation effects from the lattice components of the "apparent" or "effective" thermal conductivities reported. These apparent thermal conductivities are not intrinsic properties of the glasses. They depend on the geometry of the test specimen, the boundary conditions and can be reliably used for conditions very similar to those under which the data was gathered.

The intrinsic thermal conductivity and specific heat of float glass has only recently been determined using internal dynamic temperature measurements obtained from glass plates 0.37–1.17 cm thick. The experimental methods devised to obtain the dynamic temperature data, along with the analysis techniques necessary to extract the thermal conductivity and specific heat from the data are discussed below. The true specific heats and true thermal conductivities obtained are presented and compared with the scant applicable data available in the literature.

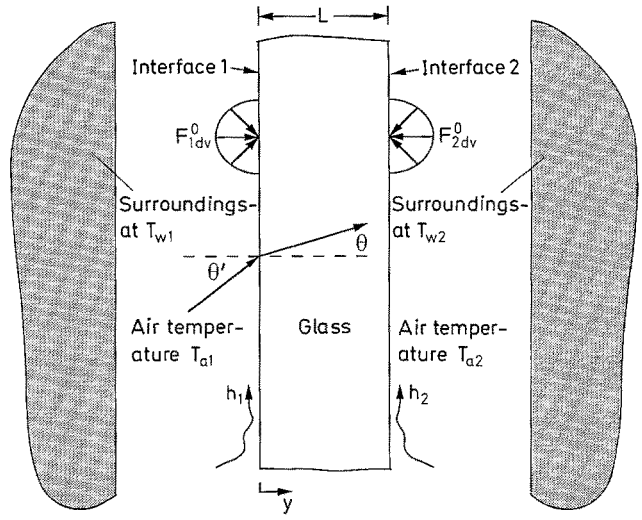

Fig. 1. Schematic of glass plate with diffuse incident flux and arbitrary convection at each interface

2 Prediction of the dynamic temperature distribution in flat glass

The formulation of the energy equation for glass must, as discussed above, properly account for the radiative energy transfer across the interfaces and throughout the interior. Radiative energy transfer modeling using rigorous radiative transfer theory was reviewed by Viskanta and Anderson [6]. The physical model of a plane layer of glass exchanging energy with the surroundings by convection and radiation is shown in Fig. 1. The following assumptions were used to develop the model equations describing this system: 1) the glass is in local thermodynamic equilibrium, therefore Planck's and Kirchhoff's laws are valid, 2) heat transfer by conduction, convection, and radiation occurs only in the y-direction normal to the plate interfaces, 3) the glass is isotropic, homogeneous, and able to absorb and emit but not scatter thermal radiation, 4) the thickness of the glass is much greater than the radiation wavelength making coherence effects negligible, 5) the glass is semitransparent to radiation for wavelengths $\lambda<\lambda_c$, and opaque for wavelengths $\lambda>\lambda_c$ [7–9], 6) the variation of the refractive index in the glass with temperature is negligible over the temperature range of 200–1000 °C compared to the variation with wavelength, and 7) the variation of radiation and thermophysical properties with wavelength and temperature are known.

The transient one-dimensional energy equation for glass is

$$\varrho\, c \frac{\partial T}{\partial t} = \frac{\partial}{\partial y}\left(k \frac{\partial T}{\partial y}\right) - \frac{\partial F}{\partial y}\,. \tag{1}$$

The expression for the radiative flux F in the y-direction is quite complex and is not given here, but it is available elsewhere [10, 11]. The solution of the energy equation requires the specification of an initial temperature distribution $T(y, 0) = T_0(y)$, and boundary conditions at each interface of the plate. The boundary conditions for Eq. (1) are obtained from an energy balance on an infinitesimal volume at the surfaces of the plate. Glass is considered semitransparent to radiation for wavelengths less than 5.0 μm. Because the volume is infinitesimal it can neither absorb or emit radiation below 5.0 μm where the emission and absorption is a volumetric phenomenon. The conduction heat transfer just beneath the surface of the glass must then equal the heat transfer just outside the glass plate due to convection and radiation above 5.0 μm. The boundary conditions at the two surfaces are:

$$k \left.\frac{\partial T}{\partial y}\right|_{y=0} = h_1 (T_{s1} - T_{a1}) + \sigma (\varepsilon_{s1} f_{s1,5-\infty\,\mu m} T_{s1}^4 - \alpha_{w1} f_{w1,5-\infty\,\mu m} T_{w1}^4)\,, \tag{2}$$

$$-k \left.\frac{\partial T}{\partial y}\right|_{y=L} = h_2 (T_{s2} - T_{a2}) + \sigma (\varepsilon_{s2} f_{s2,5-\infty\,\mu m} T_{s2}^4 - \alpha_{w2} f_{w2,5-\infty\,\mu m} T_{w2}^4)\,; \tag{3}$$

where

$$\varepsilon_{s1} = \frac{\int_{5.0\,\mu m}^{\infty\,\mu m} \varepsilon_\lambda I_{b\lambda}(T_{s1})\, d\lambda}{\int_{5.0\,\mu m}^{\infty\,\mu m} I_{b\lambda}(T_{s1})\, d\lambda}\,, \quad \varepsilon_{s2} = \frac{\int_{5.0\,\mu m}^{\infty\,\mu m} \varepsilon_\lambda I_{b\lambda}(T_{s2})\, d\lambda}{\int_{5.0\,\mu m}^{\infty\,\mu m} I_{b\lambda}(T_{s2})\, d\lambda}\,; \tag{4}$$

$$\alpha_{w1} = \frac{\int_{5.0\,\mu m}^{\infty\,\mu m} \alpha_\lambda I_{b\lambda}(T_{w1})\, d\lambda}{\int_{5.0\,\mu m}^{\infty\,\mu m} I_{b\lambda}(T_{w1})\, d\lambda}\,, \quad \alpha_{w2} = \frac{\int_{5.0\,\mu m}^{\infty\,\mu m} \alpha_\lambda I_{b\lambda}(T_{w2})\, d\lambda}{\int_{5.0\,\mu m}^{\infty\,\mu m} I_{b\lambda}(T_{w2})\, d\lambda}\,; \tag{5}$$

where $I_{b\lambda}(T)$ is Planck's black body function, and diffuse emission and irradiation is assumed.

The solution of the model equations must be accomplished using numerical procedures. The details of the numerical method and the solution sensitivity studies to deter-

mine node spacing (to obtain grid independence), time increment (to achieve time step independence), and absorption band width (to achieve spectral model band width independence) was extensively studied by Field [10] and Mann [12]. The results of these investigations indicate that spectral band width independence can be achieved with a band increment of one micron. This yields a 5 band spectral model to approximate the absorption coefficient from $\lambda=0$ to 5 μm. Node spacing independence is achieved when 5 or more nodes per millimeter are used. The implicit solution procedure used employed an iteration at each time increment to guarantee consistency between the assumed internal temperature profile and the radiative fluxes. Use of the intermediate iteration makes the solution very time-stable and insensitive to time step variations.

3 Experimental apparatus and test procedure

The test procedure used was to heat the instrumented plate to a uniform initial temperature near the softening point of the glass, and then quickly transfer it (in less than 1 s [12]) to the laboratory ambient, where its temperature distribution was monitored as it cooled. The test plates made from float glass (manufactured by the Ford Motor Co.) were fabricated in a manner which allows the placement of thermocouples both on the surface and within the interior. For these tests the thermocouples were placed on the front and rear surfaces and at the plate center plane. The test plates were sized approximately 200 mm^2, and the thermocouple junctions were positioned 12 mm from the center of the plate on the perpendicular bisector of the plate edge with a 90° clockwise rotation between each successive lateral station. A typical test plate and the thermocouple placement is shown in Fig. 2.

The approach of test plate fabrication was to fuse two glass plates into a single piece which results in the thermocouple wire being engulfed by and bonded to the glass during the fusion process. This method has the very desirable benefit, from the heat transfer point of view, that it provides optimum thermal contact between the thermocouple junction and the glass while eliminating the need for a bonding agent. Fusing the thermocouples and glass plates into an integral unit without altering the surface properties of the glass is a difficult process to accomplish. If the reflection and transmission characteristics of the surface are altered during fusion, the radiative transfer within the test plates will not be representative of glass which was not subjected to this process. Details of the fabrication process can be found in Field [10] and will not be repeated here.

The test plate was assembled by installing the center plane thermocouple and placing a tiny drop of cement at two diagonally opposite corners to hold the plates together while the surface thermocouples were installed. During the fusion process the cement decomposes and evaporates. The surface thermocouples were held in place prior to fusion

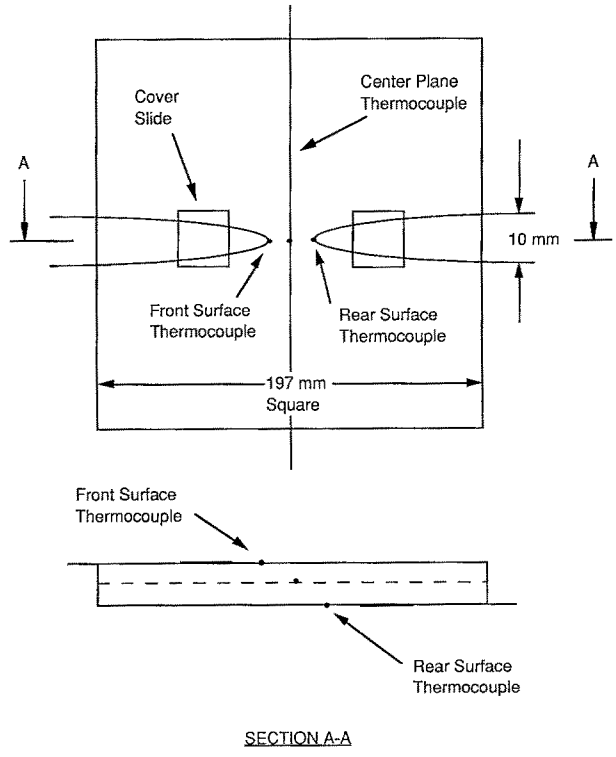

Fig. 2. Schematic of test plate

using 18 mm square by 0.5 mm thick glass cover slides also secured using a tiny drop of cement. The thermocouples were Type E Chromel-Constantan. Initially, Type K Chromel-Alumel was used, but if any moisture was present during the fusing process, the Alumel wire became very brittle [12].

4 Specific heat of glass

Primenko and Gudovich [13] measured the heat content of several glasses and proposed a method to estimate their specific heats. One of the glass compositions they examined was nearly identical to that of the float glass used in this research. Sharp and Ginther [14] also proposed an empirical equation for determining the specific heat of glass as a function of its composition.

The specific heat of glass calculated using the data of Primenko and Gudovich [13] gives a dependence on temperature similar to that of the float glass used in this investigation. The specific heat determined using their data ranged from 300° to 1500 °C. Therefore, extrapolation of the specific heat from 300 °C to room temperature was necessary. The specific heat was extrapolated using the empirical equation of Sharp and Ginther [14]. The unknowns in the empirical equation were determined by curve fitting the specific heat from 300°–550 °C determined using the Primenko and Gudovich data. Because continuity was desired, the empirical equation was made to match the specific heat at 300 °C, and a least squares best fit was used for the rest of the data.

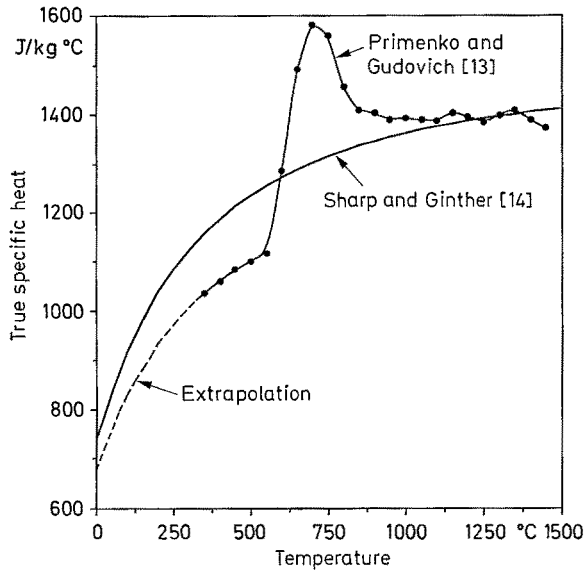

Fig. 3. Published specific heats for a particular float glass composition

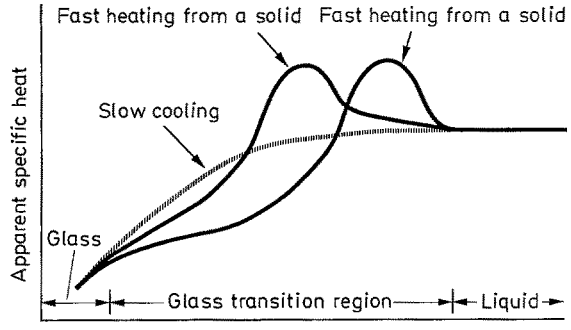

Fig. 4. Schematic representation of the apparent heat capacity on slow cooling and subsequent faster heating

The empirical equation gave an excellent fit to the specific heat for the temperatures between 300° and 550 °C and is considered a reasonable method of extrapolating to room temperature. Above 300 °C a cubic spline fit interpolation was used. The published specific heats are shown in Fig. 3.

The two specific heat curves differ significantly in shape and the magnitudes vary by as much as 25%. Investigation of the temperature dependence of the specific heat revealed interesting characteristics. The specific heat of glass through its transition region is shown in Fig. 4. The specific heat increases slowly during heating until the beginning of the transition region where a sharp increase is seen. In the transition region, the specific heat reaches a maximum, then decreases to a liquid equilibrium value. When liquid, the specific heat remains constant. Sharp and Ginther's empirical equation cannot account for transition and continually increases. The specific heat calculated using the data of Primenko and Gudovich [13] remains constant once the liquid state is reached. Small variations in the specific heat above 800 °C calculatd from their heat content data are most likely due to their experimental uncertainties.

When cooling from the liquid state, the specific heat gradually decreases and eventually meets the heating-specific heat in the solid region. There is no maximum during cooling from the liquid. No literature has been identified which describes the characteristics of the effective specific heat of glass when heated to the transition region and then cooled, as was the case for our experiments. The specific heat characteristics in the transition region are well understood, and detailed explanations can be found in the literature [15–18]. The variation of specific heat with temperature within the transition region depends on the rate of heating, the temperature, and the time at $T < T_v$. The vitrification temperature T_v, is defined as the temperature at the beginning of transition.

The specific heat is difficult to obtain within the transition region, and a procedure to determine it for each test was necessary. Assuming the change in glass temperature across the plate is small relative to the variation in glass temperature during the experiment and utilizing the definition of the specific heat, we can write

$$c_{\text{true}} = \frac{d(E/m)}{dT} \cong \frac{[h(T_{\text{air}} - T) + F_{0-5\,\mu\text{m}} + F_{5-\infty\,\mu\text{m}}]\,\Delta t/(\varrho L/2)}{\Delta T_{\text{ave}}} \tag{6}$$

or

$$c_{\text{true}} = \frac{2}{\varrho L}[h(T_{\text{air}} - T) + F_{0-5\,\mu\text{m}} + F_{5-\infty\,\mu\text{m}}] \Big/ \left(\frac{dT_{\text{ave}}}{dt}\right), \tag{7}$$

where $F_{0-5\,\mu\text{m}}$ is the radiation flux below 5.0 μm and $F_{5-\infty\,\mu\text{m}}$ is the radiation flux above 5.0 μm from the glass plate. Evaluation of Eq. (7) requires knowledge of the temperature distribution in the plate to determine the emission below 5.0 μm. The temperature distribution in the plate was assumed to be a quadratic form fit to match the surface and center thermocouple readings. The convective heat transfer coefficient on the plate surface was determined using a correlation for a vertical plate cooling in still air [19].

The uncertainty in the specific heat is related to uncertainties in the radiative fluxes in the two spectral bands and the convective heat transfer. The relative magnitudes of the three contributions are shown in Fig. 5. For temperatures above 550 °C the emission is mostly in the spectral region below 5.0 μm. Natural convection (the least well known of the three contributions) never becomes dominant. The specific heats determined from the dynamic temperature data are compared with the values from the literature in Fig. 6. The specific heat of each test plate shows remarkable consistency.

5 True thermal conductivity of glass

In solids, heat is transferred by various mechanisms including electrons, lattice waves (phonons), magnetic excitations, and in some cases electromagnetic radiation [25]. The total

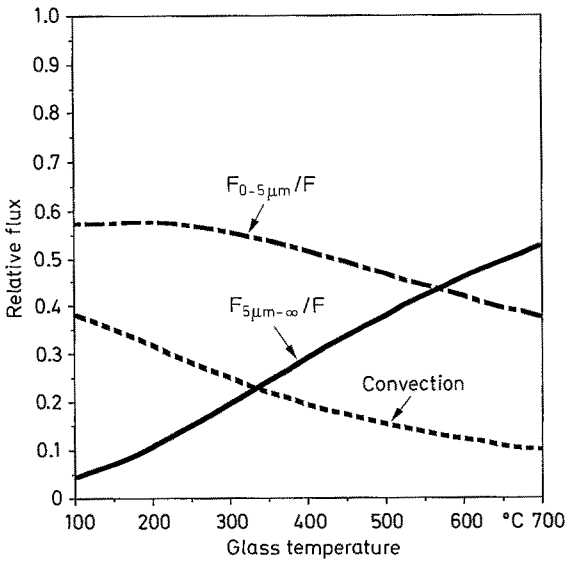

Fig. 5. Relative magnitudes of the three heat transfer contributions

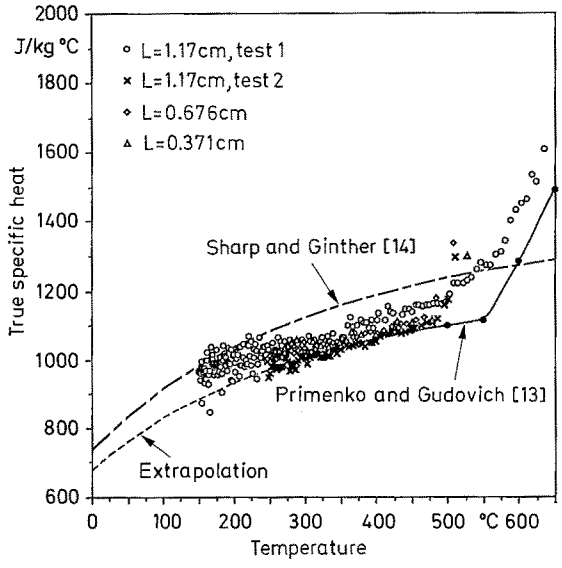

Fig. 6. Determined true specific heats of glass plates

thermal conductivity is the sum of the contribution of all types of carriers and can be expressed as

$$k = \tfrac{1}{3} \sum_i C_i v_i l_i \,. \tag{8}$$

In Eq. (8), the subscript i denotes the type of carrier, C_i is the specific heat of the solid per unit volume, v_i is the velocity of the carrier, and l_i is the suitability defined mean free path. In the electrically non-conducting, amorphous, glass (solid) heat is transferred by lattice vibrations and electromagnetic radiation. Because there is no definition (independent of geometry) of the radiative conductivity for thin glass plates, the "true" conductivity is defined here as the heat transferred due to the lattice vibrations. The dependence on temperature of the "true" thermal conductivity was predicted by Kittel [20], who suggested that the mean free path for phonons in glass is limited by geometrical effects associated with the disorder nature of the structure. Because glass has no definite order, the mean free path is independent of the phonon wavelength and phonon density. The mean free path independence then results in a thermal conductivity proportional to the specific heat [20].

A plethora of data for thermal conductivities of different glasses can be found in the thermophysical property literature [5], but as stated above, the data sources rarely make a distinction between the radiation and lattice conductivity. Two sources have been found that give a method of determining the thermal conductivity in glass due lattice vibrations. The first paper describes a method of calculating the thermal conductivity based upon the glass composition [21]. Although this method is convenient for its applicability to any glass composition, it did not correct for the radiation contribution and should be considered to give true thermal conductivity only for temperatures below 400 °C. The second paper [22], clearly defines a function based upon empirical data for the molecular (lattice) conductivity of glass. Endrys and Turzik [22] measured the total (effective) conductivity of their glass sample and subtracted the radiation contribution calculated using the absorption coefficient of the glass. The radiation conductivity was calculated using the Rosseland diffusion approximation.

The true thermal conductivity data presented in Fig. 7 for the 0.676 and 1.17 cm thick plates was determined by matching the dynamic temperature data obtained from the transient tests with the predicted temperatures from the energy model. The thermocouple readings on each side of the plate, were used as boundary conditions in the energy model solution. Using the surface temperatures as boundary conditions eliminated the need to know the convective heat transfer coefficient on the test plate surfaces. During each iteration in the energy model solution, the thermal conductivity was adjusted to match the center-plane temperature of the plate. The convergence criterion was ± 0.01 W/m °C.

The deviations in the calculated thermal conductivities from plate to plate are assumed to be from three sources. First, each test plate has a slightly different thermocouples (due to nominal alloy composition variations) causing some to read high while others may read low. For thin glass plates, the center minus the surface temperature is small, and thermocouple errors have a significant effect on the results. Only the results for the thicker plates are shown because of this effect. Two other sources of error cause deviations from the actual values. The first of these two is the dependence of absorption coefficient on temperature. The absorption coefficient has been measured and found to decrease with temperature at 3.5 μm [12]. In the energy equation model only room temperature data for the absorption coefficient was used. The actual absorption coefficients would have been slightly lower for the higher temperatures. Sensitivity studies suggest that decreases in the absorption coefficient by as much as 30% do not significantly change the values of the

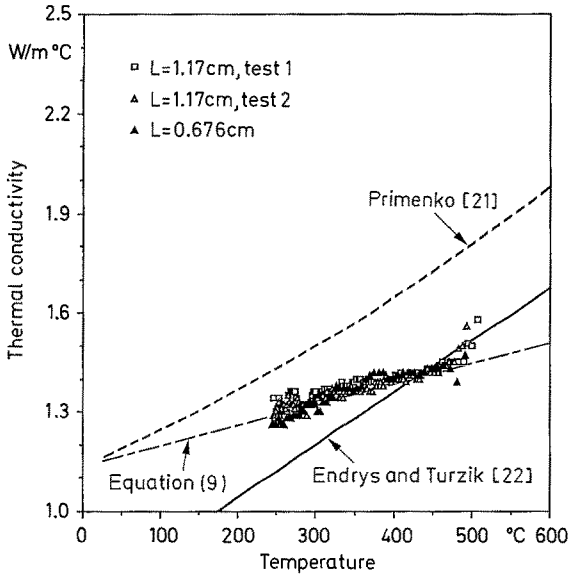

Fig. 7. Determined true thermal conductivities of glass

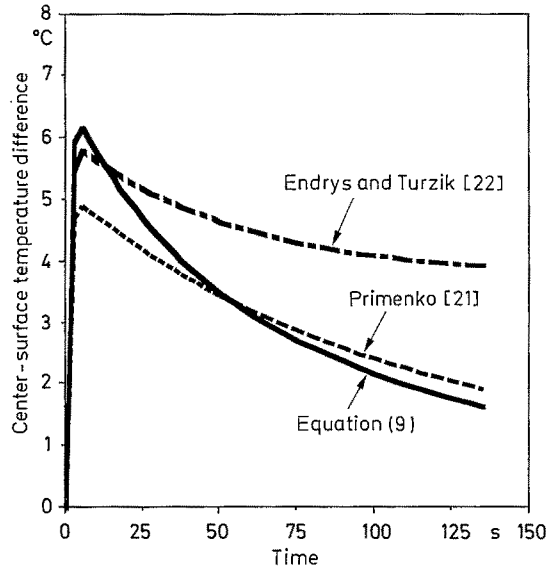

Fig. 8. Center minus surface temperatures calculated using a different thermal conductivities of glass, $L = 0.286$ cm; initial glass temperature 600 °C and natural convection from a vertical plate

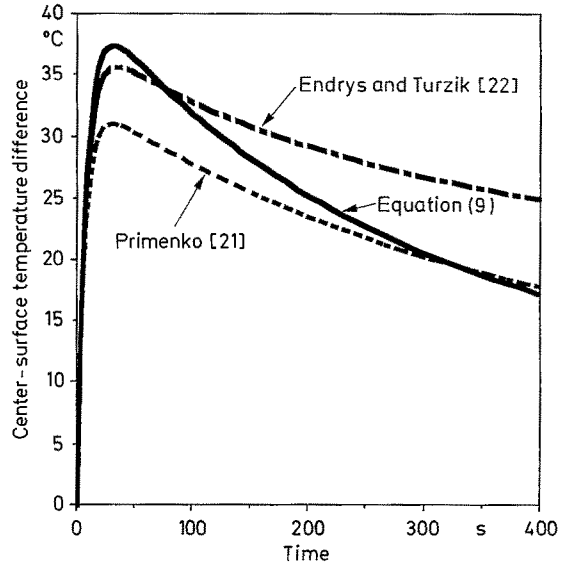

Fig. 9. Center minus surface temperatures calculated using different thermal conductivities of glass, $L = 1.27$ cm; initial glass temperature 600 °C and natural convection from a vertical plate

calculated thermal conductivity. The largest factor in the determination of the thermal conductivity is the value of specific heat. A 10% uncertainty in the specific heat will cause nearly a 20% uncertainty in the thermal conductivity. To minimize the uncertainty from the specific heat, the true thermal conductivity was determined using the specific heat measured for each test plate as discussed above. Conductivities for the thinner plates could not be satisfactorily determined due to the temperature measurement uncertainties as previously stated. The scatter in the data shown in Fig. 7 at the higher temperatures is believed to be due to the initial temperature distribution. The energy equation solution requires specification of an initial temperature distribution within the glass plate. The three measured temperatures were used to define a quadratic profile within the glass plate as the initial temperature distribution. The quadratic profile is significantly different from the actual temperature distributions very early in the transient. For the thicker plates, the quadratic profile assumption has little effect and the thermal conductivities agree well with each other.

The slope of the measured thermal conductivities with temperature does not agree with other published results. The slope shown in Fig. 7, however, is believed accurate for two reasons. First, a linear extrapolation of the thermal conductivity to room temperature gives a value at 25 °C of 1.15 W/m °C. The thermal conductivity of several pieces of the float glass were measured at the Thermophysical Properties Research Laboratory (TPRL) of Purdue University and found to be 1.15 W/m °C. Second, a linear temperature dependence of the thermal conductivity is supported by other data in the literature. For these reasons the temperature dependence of thermal conductivity of float glass is proposed to be

$$k(T) = 1.14 + 0.000624\,T \tag{9}$$

where the units of the thermal conductivity and temperature are W/mK and °C, respectively.

The correlation by Endrys and Turzik [22] for the phonon thermal conductivity of glass gives approximately 0.85 W/m °C at room temperature. This is 25% smaller than that measured for the float glass used in these experiments. At 600 °C their correlation gives a value nearly 25% greater than determined from the dynamic temperature data. The predicted center minus surface temperatures using the two correlations is shown in Figs. 8 and 9. A 25% change in

thermal conductivity will produce a 25% change in center minus surface temperature difference for a plate 0.23–1.27 mm thick.

6 Conclusions

A method to determine the true specific heat and thermal conductivity of glass and other semitransparent materials has been demonstrated. The method depends on the acquisition of dynamic internal temperature data from the surface and from within the test plate. A rigorous formulation of the energy equation model is necessary for interpretation of the data. Once these tools are available, the determination of the specific heats and thermal conductivities in semitransparent materials is a straightforward process which was shown to be simple, consistent and reliable. The limitations of the process primarily result from the simplifying assumption of a quadratic initial temperature distribution. This assumption is only troublesome for very early times in the transient temperature response with test plates which are very thin and can readily be relaxed. Hopefully, future application of this technique will eliminate much of the uncertainty in the existing specific heat and thermal conductivity data for glass and other semitransparent materials at elevated temperatures.

References

1. Barber, R.: Glass industry applications. In: Theory and practice of radiation thermometry. (Eds.: DeWitt, D. P.; Nutter, G. D.) New York: Wiley 1988, 937–1018
2. Holoman, R. A.: Mold temperature measurement for glass-pressing processes. In: Applications of radiation thermometry, ASTM STP 895. (Eds.: Richmond, J. C.; DeWitt, D. P.) Philadelphia: ASTM (1985) 67–73
3. Goodson, R. E.: Modeling for automatic control of process design. In: Proc. of the IFACS Symp. on Automatic Control in Glass. (Ed.: Mouly, R. J.) Pittsburgh: Instrument Society of America (1973) 200–209
4. Gardon, R.: Calculation of temperature distribution in glass plates undergoing heat-treatment. J. Am. Ceram. Soc. 44 (1958) 200–209
5. Touloukian, Y. S.; Powell, R. W.; Ho, C. Y.; Klemens, P. G.: Theory of thermal conductivity of nonmetallic solids. New York: IFI/Plenum 1970, 922–933
6. Viskanta, R.; Anderson, E. E.: Heat transfer in semitransparent solids. In: Advances in heat transfer. New York: Academic Press 1975, 318–441
7. Neuroth, N.: Der Einfluß der Temperatur auf die spektrale Absorption von Gläsern im Ultaroten. Glastech. Ber. 25 (1952) 242–249
8. Neuroth, N.: Der Einfluß der Temperatur auf die spektrale Absorption von Gläsern im Ultaroten II. Glastech. Ber. 26 (1953) 66–69
9. Rubin, M.: Optical properties of soda-line silica glasses. Sol. Energy Mat. 12 (1985) 275–288
10. Field, R. E.: Spectral remote sensing of the temperature distribution in glass. Ph.D. thesis, Purdue University (1989)
11. Field, R. E.; Viskanta, R.: Measurement and prediction of the dynamic temperature distributions in soda-lime glass plates. J. Am. Ceram. Soc. 73 (1990) 2047–2053
12. Mann, D. B.: Prediction and measurement of transient temperature distributions in thin glass plates. MSME thesis, Purdue University (1990)
13. Primenko, V. I.; Gudovich, O. D.: Prediction of the high-temperature specific heat of silicate glasses. Soviet J. Glass Phys. Chem. 34 (1981) 260–271
14. Sharp, D. E.; Ginther, L. B.: Effect of composition and temperature on the specific heat of glass. J. Am. Ceram. Soc. 34 (1954) 260–271
15. Morey, G. W.: The properties of glass. New York: Reinhold (1954) 210–230
16. Sharanov, Y. A.; Vol'kenshtein, M. V.: Calorimetric study of the softening and annealing of amorphous polymers. Soviet Phys. – Solid State 6 (1964) 1992–2000
17. Wolpert, M. W.; Weits, A.; Wunderlich, B.: Time-dependent heat capacity in the glass transition region. J. Polymer Science 9 (1971) 1887–1905
18. Moynihan, C. T.; Easteal, A. J.; Wilder, J.; Tucker, J.: Dependence of the transition temperature on heating and cooling rate. J. Phys. Chem. 78 (1974) 2673–2677
19. Incropera, F.; DeWitt, D. P.: Fundamentals of heat and mass transfer. New York: Wiley 1985, 424–426
20. Kittel, C.: Interpretation of the thermal conductivity of glasses. Phys. Rev. 75 (1949) 972–974
21. Primenko, V. I.: Theoretical method of determining the temperature dependence of thermal conductivity of glasses. Glass Ceram. 37 (1980) 240–242
22. Endrys, J.; Turzik, D.: Die Temperaturverteilung in Glas bei stationärem Zustand. In: 9. Internationale Baustoff- und Silikattagung Weimar, Sektion 5, Hochschule für Architektur und Bauwesen, Weimar (1985) 35–40

D. Mann
R. E. Field
R. Viskanta
Heat Transfer Laboratory
School of Mechanical Engineering
Purdue University
West Lafayette, IN 47907
USA

Received September 24, 1991